Propagation of Vortex Electron Wave Functions in a Magnetic Field

Gregg M. Gallatin
National Institute of Standards and Technology
Center for Nanoscale Science and Technology
Gaithersburg, MD 20899-6203
gregg.gallatin@nist.gov

Ben McMorran
Physics Department, University of Oregon, Eugene, OR 97403-1274

December 27, 2019

Abstract

The physics of coherent beams of photons carrying axial orbital angular momentum (OAM) is well understood and such beams, sometimes known as vortex beams, have found applications in optics and microscopy. Recently electron beams carrying very large values of axial OAM have been generated. In the absence of coupling to an external electromagnetic field the propagation of such vortex electron beams is virtually identical mathematically to that of vortex photon beams propagating in a medium with a homogeneous index of refraction. But when coupled to an external electromagnetic field the propagation of vortex electron beams is distinctly different from photons. Here we use the exact path integral solution to Schrodingers equation to examine the time evolution of an electron wave function carrying axial OAM. Interestingly we find that the nonzero OAM wave function can be obtained from the zero OAM wave function, in the case considered here, simply by multipling it by an appropriate time and position dependent prefactor. Hence adding OAM and propagating can in this case be replaced by first propagating then adding OAM. Also, the results shown provide an explicit illustration of the fact that the gyromagnetic ratio for OAM is unity. We also propose a novel version of the Bohm-Aharonov effect using vortex electron beams.

1 Introduction

Coherent beams of photons carrying axial orbital angular momentum (OAM), sometimes referred to as vortex beams, are well understood [1] [2] [3], and have various uses in optics and microscopy [4] [5] [6] [7]. Recently electron beams carrying very high amounts of axial OAM have been generated [8], and the properties of such beams have been studied [9] [11]. Mathematically the propagation of a vortex photon beam in a medium with a homogeneous index of refraction is virtually identical to that of a freely propagating vortex electron beam. This is obviously not the case when the electrons are propagating in an external electromagnetic field. Here we use the exact path integral solution to examine how an electron wave function carrying axial OAM evolves in time in a magnetic

field. We find that the propagation of a wave function carrying nonzero axial OAM is equivalent to the the propagation of a zero OAM wave function multiplied by an appropriate position and time dependent prefactor. Also, the results provide an explicit illustration of the fact the the (non-radiatively corrected) gyromagnetic ratio for OAM is unity as it must be [11]. We will see that from a practical point of view this means that the OAM vector rotates at half the rate of that the electron circulates in a magnetic field, i.e., at half the cyclotron or Landau frequency.

The paper is organized as follows Section 2 briefly reviews the derivation of the gyromagnetic ratios for orbital and spin angular momentum from the Dirac equation. Section 3 discusses the path integral solution for the (non-relativistic) propagation of the electron wave function in a magnetic field. Section 4 uses the path integral solution to study how a vortex electron beam, actually a wave packet, evolves in a magnetic and shows explicitly that the gyromagnetic ratio for OAM is unity.

2   Dirac to Schrodinger

For completeness we provide a brief review of the derivation of the Schrodinger equation from the Dirac equation which shows explicitly that the (non-radiatively corrected) gyromagnetic ratio for orbital angular momentum is unity [10].

The Dirac equation in SI units is

$$(i\gamma^\mu D_\mu - mc)\,\psi_D\,(\vec{x}, t) = 0 \tag{1}$$

where ψ_D is a four-component Dirac spinor and $D_\mu = \hbar\partial_\mu - ieA_\mu$. Here A_μ is the four-vector potential and e is the electron charge. The indices $\mu, \nu, \cdots$ take the values 0,1,2,3 which correspond to the t, x, y, z directions, respectively $x_0 = ct, x_1 = x, x_2 = y, x_3 = z$. The Einstein summation convention wherein repeated indices are summed over their appropriate range is used throughout, e.g., $u_\mu v^\mu \equiv \sum_{\mu=0}^{3} u_\mu v^\mu$.

Multiplying Eq (1) by $(i\gamma^\mu D_\mu + mc)$, and using

$$\gamma^\mu \gamma^\nu D_\mu D_\nu = D^\mu D_\mu - i\sigma^{\mu\nu}\frac{1}{2}\left[D_\mu, D_\nu\right]$$

$$= D^\mu D_\mu - \frac{1}{2}e\hbar\sigma^{\mu\nu}F_{\mu\nu} \tag{2}$$

which follows from $\{\gamma^\mu, \gamma^\nu\} = 2\eta^{\mu\nu}$ where γ^μ are the gamma matrices, $\eta^{\mu\nu}$ is the Minkowski metric, $\sigma^{\mu\nu} = (i/2)\left[\gamma^\mu, \gamma^\nu\right]$ and $F_{\mu\nu} = \partial_\mu A_\nu - \partial_\nu A_\mu$ is the field strength tensor we get [10]

$$\left(D^\mu D_\mu - \frac{1}{2}e\hbar\sigma^{\mu\nu}F_{\mu\nu} + m^2 c^2\right)\psi_D\,(\vec{x}, t) = 0 \tag{3}$$

Consider a constant magnetic field B pointing the in the z direction. Using gauge invariance we can write $A_0 = 0$, $A_1 = -\frac{1}{2}Bx_2$, $A_2 = \frac{1}{2}Bx_1$, $A_3 = 0$ or equivalently $A_i = -\epsilon_{ij3}\frac{B}{2}x_j = -\frac{B}{2}\epsilon_{ij}x_j$. Here ϵ_{ijk} and ϵ_{ij} are the totally antisymmetric Levi-Civita tensors. ϵ_{ijk} is $+1\,(-1)$ when i, j, k is an even(odd) permutation of $1, 2, 3$ and is zero otherwise and ϵ_{ij} is $+1\,(-1)$ for $i, j = 1, 2\,(2, 1)$ and is zero otherwise [10]. Note that $\partial_i A_i = 0$. We now have $F_{12} = -F_{21} = \partial_1 A_2 - \partial_2 A_1 = B$. Working in the so called "weak field limit", i.e. dropping the $\vec{A}^2$ term, gives

$$\left(\hbar^2\left(\frac{1}{c^2}\partial_t{}^2 - \partial_i{}^2\right) + ie\hbar B\left(x_1\partial_2 - x_2\partial_1\right) - e\hbar\sigma^{12}B + m^2 c^2\right)\psi_D\,(\vec{x}, t) = 0 \tag{4}$$

2

In the Dirac basis

$$\sigma^{ij} = \epsilon_{ijk} \begin{bmatrix} \sigma^k & 0 \\ 0 & \sigma^k \end{bmatrix} \tag{5}$$

where the σ^k are the Pauli matrices [10]. In terms of two-component spinors ϕ and χ, $\psi_D = \begin{bmatrix} \phi \\ \chi \end{bmatrix}$ and for a slowly moving electron (in the Dirac basis) we can set $\chi = 0$ and so finally

$$\left(\hbar^2 \left(\frac{1}{c^2} \partial_t{}^2 - \partial_i{}^2 \right) - eBL_3 - e2BS_3 + m^2c^2 \right) \phi(\vec{x}, t) = 0 \tag{6}$$

Here $L_3 = -i\hbar (x_1 \partial_2 - x_2 \partial_1)$ is the orbital angular momentum and $S_3 = \frac{\hbar}{2}\sigma^3$ is the spin angular momentum, both in the z direction. More generally [10] we can write

$$\left(\hbar^2 \left(\frac{1}{c^2} \partial_t{}^2 - \partial_i{}^2 \right) - e\vec{B} \cdot \left(\vec{L} + 2\vec{S} \right) + m^2c^2 \right) \phi(\vec{x}, t) = 0 \tag{7}$$

for a constant $\vec{B}$ field. Thus we see that the OAM, $\vec{L}$, couples to the magnetic field as $\vec{B} \cdot \vec{L}$ whereas the spin angular momentum, $\vec{S}$, couples as $2\vec{B} \cdot \vec{S}$ and so the (non-radiatively corrected) gyromagnetic ratio for orbital angular momentum $g_L = 1$ whereas for spin angular momentum $g_S = 2$. This difference has the effect that electron helicity, i.e., the spin projected in the direction of propagation, remains tangent to the trajectory, i.e, it rotates at the same rate that the electron circulates in a magnetic field. We will see below that because $g_L = 1$ this is not the case for electron beams carrying axial OAM. Note that the values of g_L and g_S are a property of the Hamiltonian and not of the wave function. The vortex wave function studied below, which carries nonzero axial OAM, still couples to the magnetic field with a g_L value of unity.

3 Path Integral Solution for Propagation in a Magnetic Field

We are interested in OAM and not spin and so we will drop the spin term in (7) and let $\phi(\vec{x}, t)$ be a single component wave function. To reduce to the nonrelativistic case substitute

$$\phi(\vec{x}, t) = e^{-imc^2t/\hbar} \psi(\vec{x}, t) \tag{8}$$

with $\psi(\vec{x}, t)$ slowly varying compared to $\exp\left[-imc^2t/\hbar\right]$ into (7) and dropping the $\partial_t{}^2 \psi$ term we get the standard Schrodinger equation

$$\left(i\hbar \partial_t + \frac{\hbar^2}{2m} \vec{\partial}^2 + \frac{e\vec{B} \cdot \vec{L}}{2m} \right) \psi(\vec{x}, t) = 0 \tag{9}$$

with $\vec{L} = -i\hbar\varepsilon_{ijk}\hat{x}_i x_j \partial_k$ where $\hat{x}_i$ is the unit vector in the i direction.

Because (9) is linear and first order in the time derivative the solution can be written in the form

$$\psi(\vec{x}, t) = \int d^3x' K(\vec{x}, t, \vec{x}', t') \psi(\vec{x}', t') \tag{10}$$

where $K(\vec{x}, t, \vec{x}', t')$ is called the "propagator" and the integral is nominally over all space. Also, the fact that (9) is first order in time allows the propagator to be written as a path integral [10] [12] [13],

3

i.e.,

$$K\left(\vec{x}, t, \vec{x}', t'\right) = \int\limits_{(\vec{x}', t')}^{(\vec{x}, t)} \delta \vec{x}\left(t\right) \exp\left[\frac{i}{\hbar} \int_{t_a}^{t_b} dt \mathcal{L}\left(\vec{x}\left(t\right), \partial_t \vec{x}\left(t\right), t\right)\right] \tag{11}$$

Here $\mathcal{L}\left(\vec{x}\left(t\right), \partial_t \vec{x}\left(t\right), t\right)$ is the classical Lagrangian corresponding to the quantum Hamiltonian, and the integral is over all paths or trajectories which go from $\vec{x}'$ at time t' to $\vec{x}$ at time t. The Lagrangian corresponding to (9) has the form

$$\mathcal{L}\left(\vec{x}\left(t\right), \partial_t \vec{x}\left(t\right), t\right) = \frac{1}{2} m \left(\partial_t \vec{x}\left(t\right)\right)^2 - e \vec{A}\left(\vec{x}\left(t\right), t\right) \cdot \partial_t \vec{x}\left(t\right) \tag{12}$$

where $\vec{A}$ is the vector potential with the magnetic field $\vec{B} = \vec{\partial} \times \vec{A}$. Using the form for $\vec{A}$ given above we get, for a constant magnetic field in the z direction,

$$\mathcal{L}\left(\vec{x}\left(t\right), \partial_t \vec{x}\left(t\right)\right) = \frac{m}{2} \left(\partial_t \vec{x}\left(t\right)\right)^2 + \frac{eB}{2} \epsilon_{ij} x_i \partial_t x_j\left(t\right) \tag{13}$$

It should be noted that the Lagrangian in (12) and (13) is the full Lagrangian, not the weak field approximation. This can be seen simply by calculating the corresponding classical Hamiltonian which yields $H = \left(\vec{p} - e\vec{A}\right)^2 / 2m$ .with $\vec{p} = m \partial_t x\left(t\right)$.

The solution for the propagator with this Lagrangian is straightforward [12] [13], indeed it's given as a problem in Feynman and Hibbs book [14]. Transform to a rotating frame with coordinated X_i in the xy or $1, 2$ plane by writing

$$x_i = \exp\left[\frac{eBt}{2m}\epsilon\right]_{ij} X_j \quad \Rightarrow \quad \begin{pmatrix} x_1 \\ x_2 \end{pmatrix} = \begin{pmatrix} \cos\left[\frac{eBt}{2m}\right] & \sin\left[\frac{eBt}{2m}\right] \\ -\sin\left[\frac{eBt}{2m}\right] & \cos\left[\frac{eBt}{2m}\right] \end{pmatrix} \begin{pmatrix} X_1 \\ X_2 \end{pmatrix} \tag{14}$$

In terms of the new variables the Lagrangian corresponds to free propagation in the z direction and a harmonic oscillator in the X_i, $i = 1, 2$ directions with radian frequency $eB/2m$. The path integral solutions for free propagation and for a harmonic oscillator are well known [12] [13]. Using these results and transforming back to the non-rotating coordinates we get

$$K\left(\vec{x}, t, \vec{x}', t'\right) = \left(\frac{m}{2\pi i \hbar T}\right)^{3/2} \frac{\frac{\omega}{2} T}{\sin\left[\frac{\omega}{2} T\right]} \exp\left[\frac{i}{2\hbar}\left(\begin{array}{c} \frac{m(z - z')^2}{T} + \frac{m\omega}{2} \cot\left[\frac{\omega}{2} T\right] \left(x_i - x_i'\right)^2 \\ + m\omega \epsilon_{ij} x_i x_j' \end{array}\right)\right] \tag{15}$$

with

$$\omega = \frac{eB}{m} \tag{16}$$

which is the standard cyclotron frequency [13] and $T \equiv t - t'$. In (15) the combination ωT always occurs divided by 2 and so we should expect various aspects of the wave function to evolve at half the rate at which the electron circulates in the magnetic field.

Note that in the limit as $\omega \to 0$ the propagator in (15) reduces to the free propagator

$$K_{free}\left(\vec{r} - \vec{r}', t - t'\right) = \left(\frac{m}{2\pi i \hbar \left(t - t'\right)}\right)^{3/2} \exp\left[\frac{im}{2\hbar} \frac{\left(x_i - x_i'\right)^2}{t - t'}\right] \tag{17}$$

which is explicitly space and time translation invariant as it should be.

4

4 Evolution of a Gaussian wave function with and without OAM

The propagator given in (15) is Gaussian in form and so if we choose a Gaussian for the wave function at $t' = 0$ it will remain Gaussian. Also, in this case the integral in (10) can be evaluated analytically.

First consider propagation perpendicular to the magnetic field. In this case let the initial normalized wave function be a Gaussian centered at the origin and propagating in the $x_2 = y$ direction

$$\psi_0\left(\vec{r}, 0\right) = \frac{1}{\sqrt{\pi\sigma^2}\sqrt{\pi L^2}} \exp\left[-\frac{x^2 + z^2}{2\sigma^2} - \frac{y^2}{2L^2} + \frac{i}{\hbar}py\right] \tag{18}$$

where we have switched from the x_i notation to the more convenient, at this stage, x, y, z notation with $\vec{r} = x\hat{x} + y\hat{y} + z\hat{z}$. This wave function is roughly σ in width in the x and z directions and has length L in the y direction. If we specify the values of ω and the radius R of the classical orbit of the electron then $p = m\omega R$. If we take σ and L to be much larger than the nominal de Broglie wavelength of $2\pi\hbar/p$ then we expect mininal "diffraction" effects to occur during propagation and as shown explicitly below this is exactly the case. This initial wave function has zero OAM about it's direction of propagation, the y direction, since

$$L_y\psi_0\left(\vec{r}, 0\right) = i\hbar\left(x\partial_z - z\partial_x\right)\psi_0\left(\vec{r}, 0\right) = 0 \tag{19}$$

To generate axial OAM the so called ladder operator approach [15] is used. Consider an operator $\mathbf{A}$ with eigenstate $|a\rangle$ such that $\mathbf{A}|a\rangle = a|a\rangle$. We now want to generate a state $|a+1\rangle$ such that $\mathbf{A}|a+1\rangle = (a+1)|a+1\rangle$. To do this we only need to find an operator $\mathbf{B}$ such that $[\mathbf{A}, \mathbf{B}] = \mathbf{B}$ since then $\mathbf{AB}|a\rangle = \mathbf{B}|a\rangle + \mathbf{BA}|a\rangle = (a+1)\mathbf{B}|a\rangle$ and so the state $\mathbf{B}|a\rangle = |a+1\rangle$, up to normalization and phase factors. Noting that

$$[L_y/\hbar, (\partial_x - i\partial_z)] = [i(x\partial_z - z\partial_x), (\partial_x - i\partial_z)] = (\partial_x - i\partial_z) \tag{20}$$

it follows that a state with 1 unit of axial OAM, $\psi_1\left(\vec{r}, 0\right)$, is given (up to normalization and phase factors) by

$$\psi_1\left(\vec{r}, 0\right) = (\partial_x - i\partial_z)\psi_0\left(\vec{r}, 0\right) = \frac{1}{\sigma^2}(-x + iz)\psi_0\left(\vec{r}, 0\right) = \frac{1}{\sigma^2}\rho e^{i\theta}\psi_0\left(\vec{r}, 0\right) \tag{21}$$

Here $\rho = \sqrt{x^2 + z^2}$ and θ increases in the counterclockwise direction when looking in the $-y$ direction and is measured from the $-x$ axis. Using the fact that $i(x\partial_z - z\partial_x) = -i\partial_\theta$ we immediately see that $L_y\psi_1 = \hbar\psi_1$.and so ψ_1 carries one unit of axial OAM. The factor of ρ, which appears automatically, is necessary since at $\rho = 0$ (= the y axis in this case) the phase $\exp[i\theta]$ is not defined and the wave function must vanish there.

5

Substituting $\psi_0(\vec{r}, 0)$ into (10) and using (15) gives

$$\psi_0(\vec{r}, t) = N \int d^3r' \exp\left[\begin{array}{c} \frac{im}{2\hbar t}(z - z')^2 + \frac{im\omega}{4\hbar}\cot\left[\frac{\omega t}{2}\right]\left((x - x')^2 + (y - y')^2\right) \\ + \frac{im\omega}{2\hbar}(xy' - yx') \\ -\frac{1}{2\sigma^2}(x'^2 + z'^2) - \frac{1}{2L^2}y'^2 + \frac{im\omega R}{\hbar}y' \end{array}\right]$$

$$= N\exp\left[\frac{im}{2\hbar t}z^2 + \frac{im\omega}{4\hbar}\cot\left[\frac{\omega t}{2}\right](x^2 + y^2)\right]$$

$$\times \int d^3r' \exp\left[\alpha_x x' + \alpha_y y' + \alpha_z z' - \frac{1}{2\beta_x}x'^2 - \frac{1}{2\beta_y}y'^2 - \frac{1}{2\beta_z}z'^2\right]$$

$$= N\exp\left[\frac{im}{2\hbar t}z^2 + \frac{im\omega}{4\hbar}\cot\left[\frac{\omega t}{2}\right](x^2 + y^2)\right]$$

$$\times \sqrt{(2\pi)^3 \beta_x\beta_y\beta_z}\exp\left[\frac{1}{2}\beta_x\alpha_x^2 + \frac{1}{2}\beta_y\alpha_y^2 + \frac{1}{2}\beta_z\alpha_z^2\right] \tag{22}$$

where

$$N = \left(\frac{m}{2\pi i\hbar t}\right)^{3/2}\frac{\frac{\omega t}{2}}{\sin\left[\frac{\omega t}{2}\right]}\frac{1}{\sqrt{\pi\sigma^2}\sqrt{\pi L^2}}$$

$$\alpha_x = -\frac{im\omega}{2\hbar}\cot\left[\frac{\omega t}{2}\right]x - \frac{im\omega}{2\hbar}y$$

$$\alpha_y = -\frac{im\omega}{2\hbar}\cot\left[\frac{\omega t}{2}\right]y + \frac{im\omega}{2\hbar}x + \frac{im\omega R}{\hbar}$$

$$\alpha_z = -\frac{im}{\hbar t}z \tag{23}$$

$$\beta_x = \left(\frac{1}{\sigma^2} - \frac{im\omega}{2\hbar}\cot\left[\frac{\omega t}{2}\right]\right)^{-1}$$

$$\beta_y = \left(\frac{1}{L^2} - \frac{im\omega}{2\hbar}\cot\left[\frac{\omega t}{2}\right]\right)^{-1}$$

$$\beta_z = \left(\frac{1}{\sigma^2} - \frac{im}{\hbar t}\right)$$

To propagate ψ_1 we can write

$$\psi_1(\vec{r}, t) = N\int d^3r' K(\vec{r}, t, \vec{r}', 0)\left(\partial_{x'} - i\partial_{z'}\right)\psi_0(\vec{r}', 0)$$

$$= \frac{N}{\sigma^2}\int d^3r' K(\vec{r}, t, \vec{r}', 0)\left(-x' + iz'\right)\psi_0(\vec{r}', 0)$$

$$= \frac{N}{\sigma^2}\partial_\lambda\int d^3r' K(\vec{r}, t, \vec{r}', 0)\exp\left[\lambda\left(-x' + iz'\right)\right]\psi_0(\vec{r}', 0)\bigg|_{\lambda=0} \tag{24}$$

The integral is still Gaussian and can be evaluated as above by letting $\alpha_x \to \alpha_x - \lambda$ and $\alpha_z \to \alpha_z + i\lambda$

6

in (22). Taking the derivative with respect to λ and setting $\lambda = 0$ then yields

$$\psi_1\left(\vec{r},t\right) = \frac{N}{\sigma^2} \exp\left[\frac{im}{2\hbar t}z^2 + \frac{im\omega}{4\hbar}\cot\left[\frac{\omega t}{2}\right]\left(x^2 + y^2\right)\right]$$

$$\times \sqrt{\left(2\pi\right)^3 \beta_x\beta_y\beta_z}\left(-\beta_x\alpha_x + i\beta_z\alpha_z\right)\exp\left[\frac{1}{2}\beta_x\alpha_x^2 + \frac{1}{2}\beta_y\alpha_y^2 + \frac{1}{2}\beta_z\alpha_z^2\right]$$

$$= \left(-\beta_x\alpha_x + i\beta_z\alpha_z\right)\frac{1}{\sigma^2}\psi_0\left(\vec{r},t\right) \tag{25}$$

with $\alpha_x, \beta_x, \ldots$ the same as in (23).

Even though both these analytic solutions can be manipulated into somewhat more convenient forms, this is not very illuminating and so we will simply plot these solutions for a set of conditions which nicely illustrate the relevant aspects of their time evolution. On the other hand it is worthwhile to examine the factor $\left(-\beta_x\alpha_x + i\beta_z\alpha_z\right)$ to get a better understanding of how it evolves and controls the orientation of the OAM. Substituting from above we find, after some algebra,

$$f\left(\vec{r},t\right) \equiv -\beta_x\alpha_x + i\beta_z\alpha_z = \frac{\cos\left[\frac{\omega t}{2}\right]x + \sin\left[\frac{\omega t}{2}\right]y}{\left(\sin\left[\frac{\omega t}{2}\right]\frac{2\hbar}{im\omega\sigma^2} - \cos\left[\frac{\omega t}{2}\right]\right)} + i\frac{z}{\left(1 - \frac{\hbar t}{im\sigma^2}\right)} \tag{26}$$

We see that $f\left(\vec{r},0\right) = -x + iz$ at $t = 0$, as it should, and that it rotates in time in the xy plane at a radian frequency of $\omega/2$. The origin of this factor is obvious. In operator notation, ignoring the $1/\sigma^2$, (21) becomes

$$|\psi_1\rangle = \left(-\mathbf{X} + i\mathbf{Z}\right)|\psi_0\rangle \tag{27}$$

The time evolution is given by

$$e^{-i\mathbf{H}t/\hbar}|\psi_1\rangle = e^{-i\mathbf{H}t/\hbar}\left(-\mathbf{X} + i\mathbf{Z}\right)|\psi_0\rangle$$

$$= \left(e^{-i\mathbf{H}t/\hbar}\left(-\mathbf{X} + i\mathbf{Z}\right)e^{+i\mathbf{H}t/\hbar}\right)e^{-i\mathbf{H}t/\hbar}|\psi_0\rangle$$

$$= f\left(\vec{\mathbf{R}},t\right)e^{-i\mathbf{H}t/\hbar}|\psi_0\rangle \tag{28}$$

where $\mathbf{H} = \left(\vec{\mathbf{P}} - e\vec{A}\left(\vec{\mathbf{R}}\right)\right)^2/2m$ is the quantum Hamiltonian corresponding to the Lagrangian (13). Note this is the full Hamiltonian, not the weak field approximation.

The position of the node of $\psi_1\left(\vec{r},t\right)$ follows from the solution to $f\left(\vec{r},t\right) = 0$. At $t = 0$ this is the y axis as shown above. For arbitrary t we have the solution

$$y = -\cot\left[\frac{\omega t}{2}\right]x$$

$$z = 0 \tag{29}$$

This solution is illustrated in Figure 1 for several values of t. This "nodal line" rotates only by π during one full period, $\tau = 2\pi/\omega$, of the electron cyclotron orbit and since this factor is the origin of the OAM carried by ψ_1 this shows explicity that the OAM rotates at half the cyclotron frequency, i.e., $g_L = 1$. This also shows that the OAM is axially oriented only at times $t = n\tau$, with $n = 0, 1, 2, \cdots$, and its direction switches between being parallel and antiparallel to the direction of propagation at each of these times.
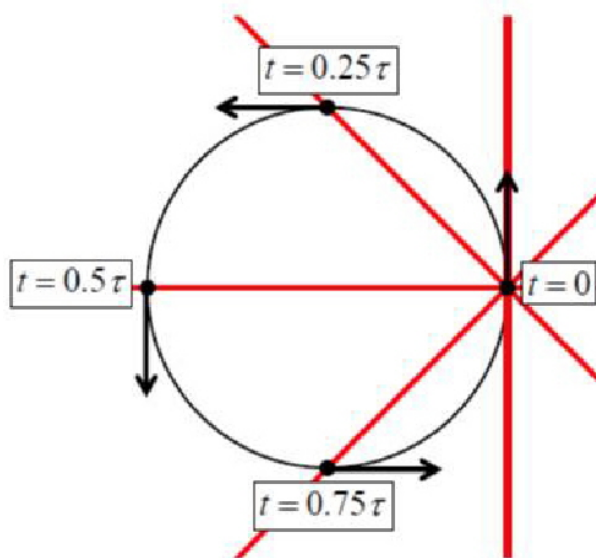
7

Figure 1: The graph shows the nodal lines (red) at different positions in the electron orbit. The OAM lies along the nodal lines and thus rotates at half the cyclotron frequency $\omega = eB/m$.

Note that $\psi_0\left(\vec{r},t\right)$ and $\psi_1\left(\vec{r},t\right)$ are not simply propagating Gaussian envelope functions multiplied by a propagating plane wave factor of the form $\exp\left[i\vec{p}\cdot\vec{r}/\hbar-iEt/\hbar\right]$ with $\left|\vec{p}\right|$ constant (but rotating at the radian frequency ω) and $E=\left|\vec{p}\right|^2/2m$. For both wave functions the de Broglie wavelength varies in time. This is to be expected since the coupling to the vector potential contributes an extra phase to the wave function of the form $-i/\hbar\int_0^t dt\vec{A}\left(\vec{r}\right)\cdot\partial_t\vec{r}\left(t\right)$ which varies with position in generally an nonlinear fashion. Figures 2 and 3 show slices of the modulus squared and the real parts of ψ_0 and ψ_1 in the xy plane at different positions in the electron orbit. The values chosen for σ,L,ω and R are such that the size of the wave packet at $t=0$, L in the y direction and σ in the x direction, are both much larger than the wavelength (so that diffraction effects are minimal) and R is much larger than L. The actual ratios used for the plots are $R=10^3L$, $L=10\sigma$ and $\sigma\simeq10^5 2\pi\hbar/m\omega$ hence the spatial range of the $\mathrm{Re}\left[\psi_0\right]$ and $\mathrm{Re}\left[\psi_1\right]$ plots is about 5 orders of magnitude smaller than for the $\left|\psi_0\right|^2$ and $\left|\psi_1^2\right|$ plots so that the phase variation is visible. In Figure 2 we see that the long axis of the wave function tracks the nodal line and the spatial extent of the wave function varies with period τ and thus the length and width return, up to diffraction effects, to their initial values at every $t=\tau$, 2τ, $3\tau,\cdots$. This periodic variation in the spatial extent of the wave function can be traced back to the fact that in the rotating frame the Lagrangian is that of a harmonic oscillator. The free propagation part of the Langrangian, $m\left(\partial_t x\right)^2/2$ causes the wave function to expand or diffract as it propagates. The harmonic oscillator part, $m\omega^2\vec{x}^2/2$ causes the wave function to contract and unless these two effects are precisely balanced the wave function will oscillate in size This is exactly analogous to the propagation of a paraxial Gaussian optical beam.centered on the z axis and propagating in the z direction in a medium with an index of refraction of the form $n\left(x,y\right)=n_0-c\left(x^2+y^2\right)$, i.e, a harmonic osciallator potential. In the paraxial approximation the propagator for the photon beam has the same Gaussian form as the propagator for the harmonic oscillator. The quadratic variation of the index of refraction will cause the beam to focus or shrink in size as it propagates whereas diffraction effects cause the beam to expand as it propagates. If the beam is large, so that the focusing effect dominates, then the beam will shrink in size as it propagates. Eventually it reaches a size where the diffraction effect dominates and it begins to expand. This process repeats itself causing the beam to oscillate in size with a fixed period along its length [16]. These oscillations can be prevented if the size of the beam is fine tuned so that the diffraction and focusing effects exactly cancel out [16]. Figure 3 shows the propagation of the wave function ψ_1 carrying a single unit of OAM. The node in the center of the wave function maintains its alignment on the nodal line during each cycle. The spiral form the phase of ψ_1 is apparent in the $\mathrm{Re}\left[\psi_1\right]$ plots. Clearly the OAM is rotating at half the cyclotron frequency ω.

Now consider propagation parallel to the magetic field. In this case we let

$$\psi_0\left(\vec{r},0\right)=\frac{1}{\sqrt{\pi\sigma^2}\sqrt{\pi L^2}}\exp\left[-\frac{x^2+y^2}{2\sigma^2}-\frac{z^2}{2L^2}+\frac{i}{\hbar}pz\right] \tag{30}$$
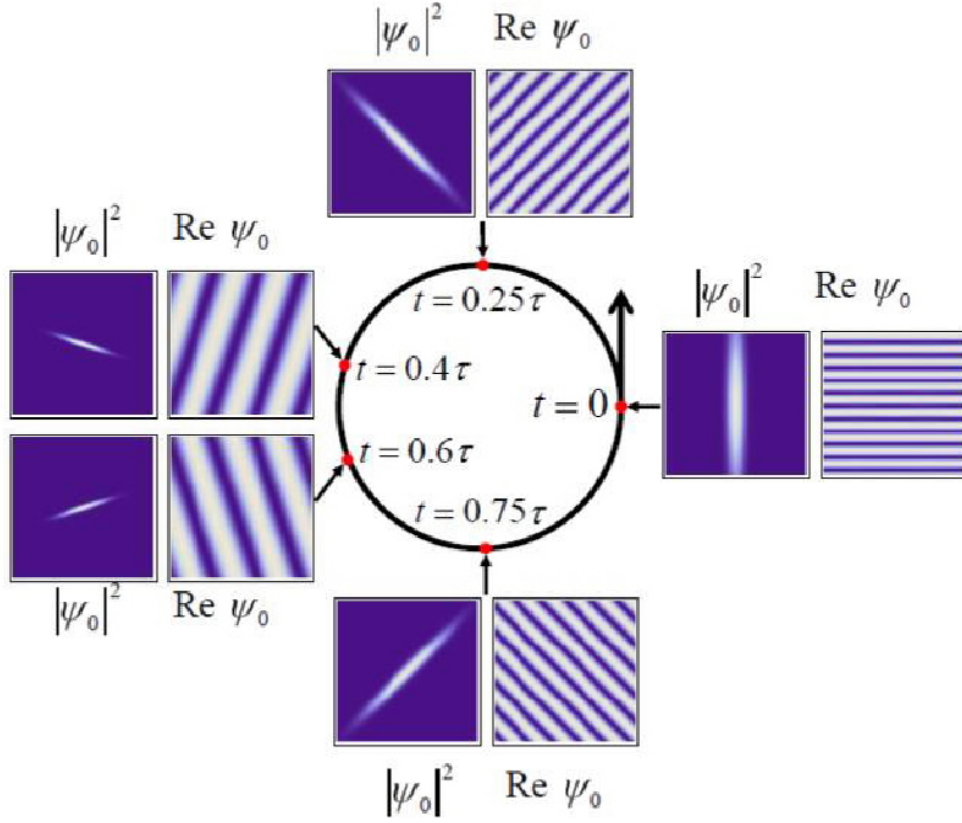
9

Figure 2: Slices in the xy plane of $|\psi_0|^2$ and Re $[\psi_0]$ at different positions around the cyclotron orbit where ψ_0 is a Gaussian wavepacket carrying 0 axial orbital angular momentum(OAM). The values chosen for the width σ and length L of the wavepacket, the cyclotron frequency $\omega = eB/m$, and the radius of the cycloctron orbit R are such that the size of the wave packet at $t = 0$ (L in the y direction and σ in the x direction) are much larger than the wavelength so that diffraction effects are minimal. All the plots are the same fixed spatial scale with that of the Re $[\psi_0]$ plots being about 5 orders of magnitude smaller than the $|\psi_0|^2$ plots so that the phase of the wavepacket is visible. At $t = 0.5\tau$ the wavepacket would be too small to be seen at this fixed spatial scale and so it is shown at times $t = 0.4\tau$ and $t = 0.6\tau$ instead.
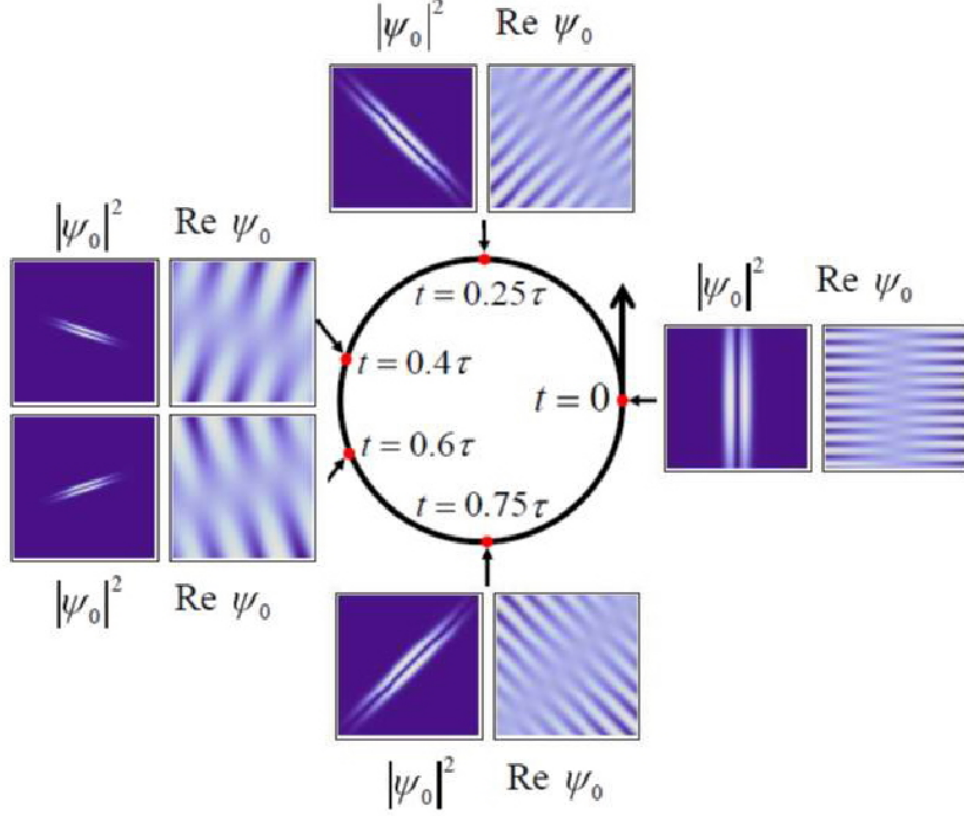
Figure 3: Slices in the xy plane of $|\psi_1|^2$ and Re $[\psi_1]$ at different positions around the cyclotron orbit where ψ_1 is a Gaussian wavepacket carrying 1 unit axial orbital angular momentum(OAM) oriented in the y direction at $t = 0$. The values chosen for the width σ and length L of the wavepacket, the cyclotron frequency $\omega = eB/m$, and the radius of the cycloctron orbit R are the same as in Figure 2, i.e., they are such that the size of the wave packet at $t = 0$ (L in the y direction and σ in the x direction) are much larger than the wavelength so that diffraction effects are minimal. All the plots are the same fixed spatial scale with that of the Re $[\psi_1]$ plots being about 5 orders of magnitude smaller than the $|\psi_1|^2$ plots so that the phase of the wavepacket is visible. At $t = 0.5\tau$ the wavepacket would be too small to be seen at this fixed spatial scale and so it is shown at times $t = 0.4\tau$ and $t = 0.6\tau$ instead.

and

$$
\begin{aligned}
\psi_0\left(\vec{r}, t\right) &= N \int d^3 r' \exp\left[\begin{array}{c} \frac{im}{2\hbar t}\left(z - z'\right)^2 + \frac{im\omega}{4\hbar}\cot\left[\frac{\omega t}{2}\right]\left(\left(x - x'\right)^2 + \left(y - y'\right)^2\right) \\ + \frac{im\omega}{2\hbar}\left(xy' - yx'\right) \\ -\frac{1}{2\sigma^2}\left(x'^2 + y'^2\right) - \frac{1}{2L^2}z'^2 + \frac{ip}{\hbar}z' \end{array}\right] \\
&= N \exp\left[\frac{im}{2\hbar t}z^2 + \frac{im\omega}{4\hbar}\cot\left[\frac{\omega t}{2}\right]\left(x^2 + y^2\right)\right] \\
&\quad \times \int d^3 r' \exp\left[\alpha_x x' + \alpha_y y' + \alpha_z z' - \frac{1}{2\beta_\rho}\left(x'^2 + y'^2\right) - \frac{1}{2\beta_z}z'^2\right] \\
&= N\sqrt{\left(2\pi\right)^3 \beta_\rho{}^2 \beta_z} \\
&\quad \times \exp\left[\begin{array}{c} \left(\frac{im\omega}{4\hbar}\cot\left[\frac{\omega t}{2}\right] - \frac{1}{2}\beta_\rho\left(\frac{m\omega}{2\hbar\sin\left[\frac{\omega t}{2}\right]}\right)^2\right)\left(x^2 + y^2\right) \\ -\beta_z\left(\frac{m}{\hbar t}\right)^2\left(z - \frac{p}{m}t\right)^2 + \frac{im}{2\hbar t}z^2 \end{array}\right]
\end{aligned}
\tag{31}
$$

where N is the same as in (23) but now

$$
\beta_\rho = \left(\frac{1}{\sigma^2} - \frac{im\omega}{2\hbar}\cot\left[\frac{\omega t}{2}\right]\right)^{-1}
$$

$$
\beta_z = \left(\frac{1}{L^2} - \frac{im}{\hbar t}\right)
\tag{32}
$$

Because $\psi\left(\vec{r}, t\right)$ depends on x and y only in the combination $\rho^2 = x^2 + y^2$ it follows that the initial Gaussian wave function chosen here does not pick up angular momentum as it propagates along the magnetic field. In fact for propagation parallel to the magnetic field the axial OAM of an eigenstate of $\mathbf{L}_z$ is conserved. This follows directly from

$$
[\mathbf{L}_z, \mathbf{H}] = 0
\tag{33}
$$

where again $\mathbf{H} = \left(\vec{\mathbf{P}} - e\vec{A}\left(\vec{\mathbf{R}}\right)\right)^2 / 2m$ and $\mathbf{A}_i = -\frac{B}{2}\epsilon_{ij}\mathbf{X}_j$. Indeed it can be shown that $\mathbf{H} = \frac{1}{2m}\vec{\mathbf{P}}^2 - \frac{eB}{2m}\mathbf{L}_z + \frac{e^2 B^2}{2m}\left(\mathbf{X}^2 + \mathbf{Y}^2\right)$ which obviously yields (33).

5   Conclusion

Using the exact path integral solution for the propagator in a constant magnetic field we have derived the evolution of a Gaussian wave function and shown explicitly that the (non-radiatively corrected) gyromagnetic ratio g_L for OAM is unity. This must be the case since g_L is a property of the Hamiltonian and not of the wave function.

The results presented above lead to a novel version of the Aharonov-Bohm effect [17]. Consider a long thin solenoid aligned along the z axis. Outside the solenoid (far from the ends) $\vec{A}$ varies as $1/\rho = 1/\sqrt{x^2 + y^2}$ and so $\vec{B}$ is zero outside. Inside the solenoid $\vec{A}$ varies as ρ and so $\vec{B}$ is constant and nonzero. A Gaussian wave function like those considered above carrying nozero OAM that propagates along the z axis has a node on the z axis. In fact wave functions carrying large values of

OAM have a very large region around the z axis where the wave function is effectively zero [8]. As in the standard Aharonov-Bohm experiment [17] this is a case where there is no overlap between the wave function and the magnetic field. The wave function only overlaps with the magnetic vector potential. Hence the presence of the solenoid will cause a change in how the wave function propagates relative to the no solenoid case. This effect will be predominantly a change in the focus position of the wave function. Experimental verification of this would provide yet another example of the fact A_μ is the fundamental quantity and not $\vec{E}$ and $\vec{B}$.

References

[1] Mark R. Dennis, Kevin O'Holleran, Miles J. Padgett, "Singular Optics: Optical Vortices and Polarization Singularities", Chapter 5, Progress in Optics, vol. 53, 293-363, Elsevier (2009).

[2] Miles Padgett, Johannes Courtial and Les Allen, "Light's Angular Momentum", Physics Today, May 2004, p 35.

[3] U. D. Jentschura and B. G. Serbo, "Generation of High-Energy Photons with Large Orbital Angular Momentum by Compton Backscattering", Phys. Rev. Letts. **106**, 013001 (2011).

[4] Sri Rama Prasanna Pavani and Rafael Peistun, "High-efficiency rotating point spread functions", Opt. Exp. **16**, 3484 (2008).

[5] Gabriel Molina-Terriza, Juan P. Torres, and Lluis Torner, "Twisted Photons", Nat. Phys. **3**, p. 305 (2007).

[6] Sri Rama Prasanna Pavani, Michael A. Thompson, Julie S. Biteen, Samuel J. Lord, Na Liu, Robert J. Twieg, Rafael Piestun and W. E. Moerner, "Three-dimensional, single-molecule fluorescence imaging beyond the diffraction limit by using a double-helix point spread function", PNAS **106**, p. 2995 (2009).

[7] Michael A. Thompson, Matthew D. Lew, Majid Badieirostami and W. E. Moerner, "Localizing and Tracking Single Nanoscale Emitters in Three Dimensions with High Spatiotemporal Resolution Using a Double-Helix Point Spread Function", Nano Lett. **10**, p. 211 (2010).

[8] Benjamin J. McMorran, Amit Agrawal, Ian M. Anderson, Andrew A. Herzing, Henri J. Lezec, Jabez J. McClelland, and John Unguris, "Electron Vortex Beams with High Quanta of Orbital Angular Momentum", Science **331**, p 192 (2011).

[9] J. Verbeek, H. Tian, and P. Schattschneider, "Production and application of electron vortex beams", Nature **467**, p. 301 (2010).

[10] A. Zee, *Quantum Field Theory in a Nutshell*, Chapter III.6, 2nd ed., Princeton University Press (2010).

[11] Konstantin Yu. Bliokh, Mark R. Dennis and Franco Nori, "Relativistic Electron Vortex Beams: Angular Momentum and Spin-Orbit Interaction", Phys. Rev. Lett. **107**, 174802 (2011).

[12] Richard P. Feynman, Albert R. Hibbs, and Daniel F. Styer, *Quantum Mechanics and Path Integrals: Emended Edition*, Dover Publications (2010).

[13] Hagen Kleinert, *Path Integrals in Quantum Mechanics, Statistics, Polymer Physics, and Financial Markets*, Chapter 2.18, World Scientific Publishing Company (2009).

[14] Richard P. Feynman, Albert R. Hibbs, and Daniel F. Styer, *Quantum Mechanics and Path Integrals: Emended Edition*, Problem 3-10, Dover Publications (2010).

[15] see for example, J. J. Sakurai and Jim J. Napolitano, *Modern Quantum Mechanics*, 2nd edition, Addison Wesley (2010).

[16] see for example, Amnon Yariv and Pochi Yeh, *Optical Waves in Crystals: Propagation and Control of Laser Radiation*, Chapter 2, Wiley-Interscience (2002).

[17] see for example, A. Zee, *Quantum Field Theory in a Nutshell*, Chapter IV.4, 2nd ed., Princeton University Press (2010).